Evidence for Suppressed Screening on the Surface of High Temperature $La_{2-x}Sr_xCuO_4$ and $Nd_{2-x}Ce_xCuO_4$ Superconductors

M. Taguchi,[1] A. Chainani,[1] K. Horiba,[1] Y. Takata,[1] M. Yabashi,[2,3] K. Tamasaku,[2] Y. Nishino,[2] D. Miwa,[2] T. Ishikawa,[2] T. Takeuchi,[1] K. Yamamoto,[1] M. Matsunami,[1] S. Shin,[1,4] T. Yokoya,[3] E. Ikenaga,[3] K. Kobayashi,[3] T. Mochiku,[5] K. Hirata,[5] J. Hori,[6] K. Ishii,[6] F. Nakamura,[6] and T. Suzuki[6]

[1]*Soft X-ray Spectroscopy Laboratory, RIKEN/SPring-8, Mikazuki, Mikazuki, Hyogo 679-5148, Japan*
[2]*Coherent X-ray Optics Laboratory, RIKEN/SPring-8, Mikazuki, Mikazuki, Hyogo 679-5148, Japan*
[3]*JASRI/SPring-8, Mikazuki, Mikazuki, Hyogo 679-5198, Japan*
[4]*Institute for Solid State Physics, University of Tokyo, Kashiwa, Chiba 277-8581, Japan*
[5]*Superconducting Materials Center, National Institute for Materials Science, Tsukuba, Ibaraki 305-0047, Japan*
[6]*Department of Quantum Matter, ADSM, Hiroshima University, Higashi-Hiroshima, Hiroshima 739-8530, Japan*

(Received 26 January 2005; published 19 October 2005)

Hard x-ray photoemission spectroscopy (PES) of Cu core electronic states, with a probing depth of ~60 Å, is used to show that the Zhang-Rice singlet feature is present in La_2CuO_4 but is absent in Nd_2CuO_4. Hole and electron doping in $La_{2-x}Sr_xCuO_4$ (LSCO) and $Nd_{2-x}Ce_xCuO_4$ (NCCO) result in new well-screened features which are missing in soft x-ray PES. Impurity Anderson model calculations establish screening from doped states as its origin, which is strongly suppressed within 15 Å of the surface. Complemented with x-ray absorption spectroscopy, the small chemical-potential shift in core levels (~ 0.2 eV) are shown to be consistent with modifications of valence and conduction band states spanning the band gap (~ 1 eV) upon hole and electron doping in LSCO and NCCO.

DOI: 10.1103/PhysRevLett.95.177002 PACS numbers: 74.72.Dn, 74.72.Jt, 78.20.Bh, 79.60.−i

Hole (h) and electron (e) doping by chemical substitutions in single layer copper-oxides (as in $La_{2-x}A_xCuO_4$, A = Ba, Sr, and $Nd_{2-x}Ce_xCuO_4$) transforms an antiferromagnetic insulator to an exotic metal with superconductivity [1]. The properties of h and e doped high-T_c cuprates are determined by electronic states near the chemical potential (CP) [1], accompanied with characteristic features in core levels [2]. Soft x-ray (SX, $h\nu \sim 1000$–1500 eV) core level photoemission spectroscopy (PES) with a probing depth of ~10–15 Å is valuable in studying valence change, CP shift, and screening effects in solids [3]. Combinations of core level PES with model calculations have been used to describe the parent insulating cuprates La_2CuO_4 (LCO) and Nd_2CuO_4 (NCO) as charge-transfer insulators in the Zaanen-Sawatzky-Allen classification scheme [4], with the on-site Coulomb energy (≈8 eV), being much larger than the charge transfer energy (≈2 eV) between the O $2p$ and Cu $3d$ states [5–8].

$La_{1.85}Sr_{0.15}CuO_4$ (LSCO) and $Nd_{1.85}Ce_{0.15}CuO_4$ (NCCO) are prototypical of h and e doped cuprates and exhibit a $d_{x^2-y^2}$ superconducting gap. The normal phase resistivity ($\rho \propto T^2$) is like a Fermi liquid for NCCO [9], but non-Fermi-liquid-like ($\rho \propto T$) for LSCO [10]. The strong correlations lead to special spectral behavior such as nonlocal screening effects [11,12], and anomalous spectral weight transfer upon doping [13]. While valency and CP changes in the high-T_c cuprates can be probed with SX-PES, in spite of several core level and valence band (VB) PES studies, there remains a seemingly simple and yet unresolved puzzle about the doping dependent electronic structure of the high-T_c cuprates [5–8,12–16]. The puzzle involves distinguishing between the ''midgap pinning'' or ''crossing the gap'' scenario to simultaneously explain changes in core levels and VBs. The midgap pinning scenario [5,6,15,16] involves formation of new states within the band gap on h and e doping. It explains the small CP shift of −0.2 eV (or +0.2 eV) in O $1s$ core level PES of LSCO (or NCCO) compared to undoped LCO (or NCO), but is inconsistent with the large optical gap onset (~1.0 eV) of the insulating parents [17]. In an alternative picture, the CP moves to the top of the VB by h doping and the bottom of the conduction band on e doping. Using resonant PES [14], it was shown that e and h doping leads to a crossing of the gap (~1.0 eV) from NCCO to LSCO. However, the small CP shift in O $1s$ core levels cannot be explained by this scenario.

While many Cu $2p$ core level SX-PES of LSCO and NCCO have been performed, the spectra show very little change upon doping [5–8,16]. This leads to another significant issue: the presence of the predicted Zhang-Rice singlet (ZRS) in Cu $2p$ PES of the insulating cuprates [11,12], which is considered very important for superconductivity but has not been observed to date by core level PES. However, recent spin-polarized resonant VB-PES studies distinguish between LSCO and NCCO: the ZRS survives in LSCO [18] but is absent in NCCO [19]. These puzzles bring into question the role of the depth sensitivity of PES, which has often led to controversies regarding surface versus bulk electronic structure. Pioneering core level PES with a photon energy of 8 keV (probing depth ~80 Å) was reported 30 years ago [20], but its importance for separating the surface and bulk electronic structure was recognized only recently [21].

In an attempt to describe all the spectroscopic physics correctly, we carry out core level hard x-ray (HX) PES [22,23] of single-crystal e doped NCCO, h doped LSCO, and undoped NCO and LCO. The kinetic energy of the Cu $2p$ level corresponds to a probing depth of $\sim$60 Å as determined by the inelastic mean free path [3]. Single crystals of NCO, NCCO, LCO, and LSCO are grown by the traveling solvent floating zone method. NCCO and LSCO show a superconducting T_c of 22 K and 36 K, respectively. HX-PES is performed using a photon energy $h\nu = 5.95$ keV, at a vacuum of 1×10^{-10} Torr. The measurements are carried out at undulator beam line BL29XU, SPring-8 [22]. The HX-PES instrumentation details are described in Ref. [24]. SX-PES ($h\nu = 1.5$ keV) is performed at BL17SU, with $\Delta E \sim 0.3$ eV. All measurements use a normal emission geometry to maximize depth sensitivity. All samples are fractured *in situ*. NCCO and LSCO are measured at 35 K while LCO and NCO were measured at room temperature. Gold $4f$ levels are measured to calibrate the energy scale.

Figure 1(a) shows Cu $2p_{3/2}$ HX-PES spectra and SX-PES ($h\nu = 1.5$ keV) of NCCO, LCO, and LSCO. Figure 1(b) shows the Cu $2p_{3/2}$ HX-PES spectra of undoped NCO, LCO, and h doped LSCO. The NCO Cu $2p_{3/2}$ spectrum consists of a main peak at 933.5 eV ($2p^5 3d^{10}\underline{L}$ state: $\underline{L}$ represents the ligand hole) and a broad satellite centered at 943 eV ($2p^5 3d^9$ state), and is very similar to earlier SX-PES [7,8]. The HX-PES spectra of NCCO, LCO, and LSCO [Figs. 1(a) and 1(b)] are clearly different and provide new results:

(i) The LCO HX-PES spectrum [Fig. 1(b)] shows a main peak at $\sim$932 eV and a shoulder at $\sim$933.5 eV. Using a multisite cluster model (MSCM) [11,12,25], it was shown that even for the insulating parent, the Cu $2p_{3/2}$ spectrum has a low binding energy (BE) ZRS feature due to nonlocal screening, while the $2p^5 3d^{10}\underline{L}$ state occurs at higher BE. But earlier SX-PES showed only a single peak at 933.5 eV due to the $2p^5 3d^{10}\underline{L}$ state. HX-PES clearly shows that, in LCO, the peak at 933.5 eV is the $2p^5 3d^{10}\underline{L}$ and the new feature at $\sim$932 eV is the ZRS peak. This is the first observation of the ZRS feature in Cu $2p$ PES of LCO. The ZRS feature is missing in the NCO HX-PES [Fig. 1(b)]. In $Sr_2CuO_2Cl_2$, a model insulating compound of the cuprates, the well-screened main peak consists of multiple components, and theory including local screening and nonlocal screening underestimates the width of the main peak [8,26].

(ii) The LSCO spectrum [Fig. 1(b)] shows clear changes compared to LCO. The ZRS feature is retained on h doping, but is weakened compared to LCO, and additional spectral weight is seen at higher BE (feature β). Since the main peak width (nearly 4 eV) is very large in LSCO, it consists of more than a single state ($2p^5 3d^{10}\underline{L}$ and β features). While the doping is supposed to cause a valency change (Cu^{3+} content due to h doping), it is impossible to separate out the Cu^{3+} and retained ZRS features, from the

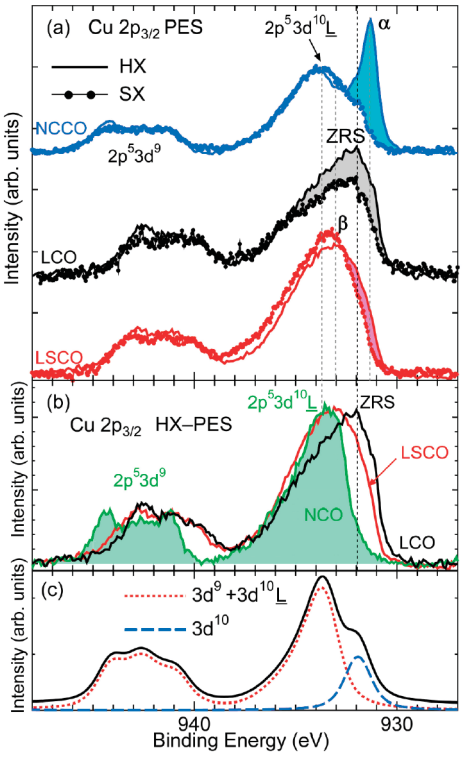

FIG. 1 (color). (a) Comparison between experimental Cu $2p$ HX-PES (solid line) and SX-PES (line with symbols) for e doped NCCO, undoped LCO, and h doped LSCO. Shaded regions highlight the differences in HX-PES. (b) Experimental Cu $2p$ HX-PES comparison of NCO, LCO, and LSCO. (c) Calculated spectra with $3d^9 + 3d^{10}\underline{L}$ (dotted line, represents the NCO spectrum) and with $3d^{10}$ (dashed line).

$2p^5 3d^{10}\underline{L}$ feature. Within experimental accuracy, the $2p^5 3d^{10}\underline{L}$ feature in all the materials occurs at the same position ($\pm$0.1 eV) as in the SX-PES data [5–8].

(iii) The HX-PES for NCCO [Fig. 1(a)] shows a sharp low BE feature α which is not observed in NCCO SX-PES as well as NCO HX-PES. Its energy position is different from the ZRS feature in LCO. More importantly, since the ZRS feature is missing in undoped NCO, its origin is different and discussed in the framework of the impurity Anderson model (IAM) later. For the same sample and surface preparation (single-crystal cleaved surfaces), SX-PES shows a peak at $\sim$933.5 eV and a weak shoulder at $\sim$932.0 eV. The SX-PES is very similar to a recent report, with the $2p^5 3d^{10}\underline{L}$ state at $\sim$933.5 eV and a weak shoulder due to the $2p^5 3d^{10}$ state [14]. In terms of the Ce content ($x = 0.15$), a maximum of 15% of the spectral intensity can arise due to the formally Cu^{1+} $3d^{10}$ state, in contrast to the observed intensity ($\sim$30%). We calculated spectra for NCO (using $3d^9 + 3d^{10}\underline{L}$ states) in the IAM [8], and for NCCO (using a linear combination of $3d^9 + 3d^{10}\underline{L}$ and $3d^{10}$ states with a relative weight of 85% and 15%), respectively, [Fig. 1(c)]. A relative energy shift between $3d^{10}\underline{L}$ and $3d^{10}$ states of 1.5 eV is used, as is known from experiments of CuO (Cu^{2+}) and Cu_2O (Cu^{1+}) [27]. While the calculation for NCO matches the data, the calculated

intensity of feature α does not match the experimental HX-PES data for NCCO. This indicates that a simple $3d^{10}$ state due to e doping cannot explain the observed high intensity of feature α.

(iv) The "ZRS," "α," and "β" features in LCO, NCCO, and LSCO [Fig. 1(a)] are clearly observed in HX-PES, respectively. While these features are missing in earlier SX-PES [5–8,16], we find evidence for the ZRS feature in LCO and broadening in LSCO even in SX-PES measurements carried out on high-quality single crystals fractured *in situ*. Also, the satellite features between NCCO and NCO show little change with doping, and so also for LSCO and LCO. The small changes in the satellite intensity between SX- and HX-PES is consistent with a modified crystal field splitting on the surface compared to bulk, as discussed by Boske *et al.* [26]. However, since the well-screened main peak features correspond to a fully filled $3d^{10}$ state, it has a different origin [26]. A large shift of nearly 1.5 eV to higher BE is observed for the NCO/NCCO satellite compared to LCO/LSCO.

While the Cu $2p$ HX-PES spectra are significantly different compared to SX-PES spectra, the O $1s$ core level HX-PES spectra are very similar to the SX-PES spectra [Fig. 2(a)]. The O $1s$ levels show a shift in peak position towards higher BE (+0.25 eV) in the e doped NCCO and towards lower BE in the h doped LSCO (−0.2 eV), in accord with earlier SX-PES studies [7,8,16]. Generally, it is believed that these shifts may reflect the CP shift.

The above described experimental results using HX-PES for undoped and doped cuprates can be explained by MSCM with a nonlocal screening effect [11,12]. In particular, the ZRS state observed in LCO, the h doping-induced changes in LSCO, and the feature α in e doped NCCO can be explained by MSCM as shown earlier [11,12]. In the MSCM, h doping decreases the nonlocal screening or ZRS with respect to local screening and would explain the observed line shape and transfer of spectral weight to higher BE upon h doping. However, from the present work, we find that NCO (the undoped parent for the e doped system) does not show the ZRS feature [Fig. 1(b)].

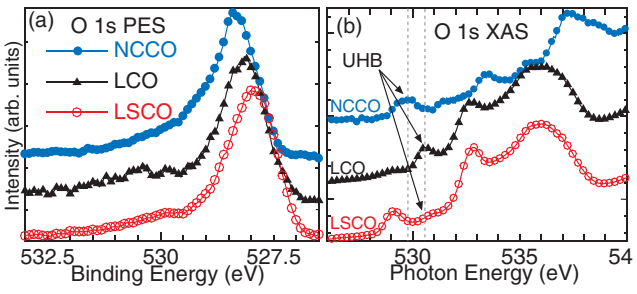

FIG. 2 (color). O $1s$ HX-PES spectra (a) and O $1s$ XAS spectra (b) of NCCO, LCO, and LSCO. The relative position of the UHB with respect to the O $1s$ core level in LSCO and NCCO can be estimated from the O $1s$ XAS. The O $1s$ XAS shows a "pre-peak" feature due to the UHB that is brought about by O $2p$-Cu $3d$ hybridization.

Since the IAM calculation works for NCO [Fig. 1(c)], and the calculations are simpler than MSCM calculations, we attempted its validity in the present case, although it is clear that our model cannot reproduce the ZRS feature in LCO. IAM calculations with the doping-induced state are performed in the D_{4h} local symmetry including intra-atomic multiplets. Here we retain only a single Cu atom (core-hole site) and allow charge transfer between the Cu $3d$ state and the O $2p$ band as well as the Cu $3d$ state and doping-induced states. The essential new feature is the charge transfer from doping-induced states to the upper Hubbard band (UHB) Δ^* defined as $E(3d^{10}\underline{C}) - E(3d^9)$. The usual charge transfer energy (from the O $2p$ band to UHB), is defined as $E(3d^{10}\underline{L}) - E(3d^9)$. The $3d^{10}\underline{C}$ represents the charge transfer between Cu $3d$ state and the doping-induced state at E_F. The O $2p$ bands and doping-induced states ε_k are approximated by $N(= 13)$ discrete levels and the k dependence of the hybridization is assumed to be elliptical. The technical details of the calculation have been reported in Refs. [24,28,29]. It was also shown that the IAM with doping-induced states mimics the nonlocal screening of the MSCM, albeit due to an *ad hoc* inclusion of doping-induced states [24].

The calculated and experimental results are shown in Fig. 3 for LSCO and NCCO. The calculations reproduce well the main peaks and satellite structure. It is known that the intensity ratio of the well-screened peak to the poorly-screened satellite is determined by the effective Δ [26]. The sharp peak at low BE in NCCO originates from core-hole screening by doping-induced states at E_F, the $2p^5 3d^{10}\underline{C}$ state. The obtained parameter values show small differences for LSCO and NCCO as summarized in Table I. The most important parameter is Δ^*, which represents the energy difference between the UHB and doping-induced states. The small value of $\Delta^*(= 0.25$ eV) for NCCO indicates that the doping-induced states lie just below the UHB, whereas a large $\Delta^*(= 1.35$ eV) of LSCO describes the situation for doping-induced states lying near the top of the VB, with the UHB separated by Δ^*. How-

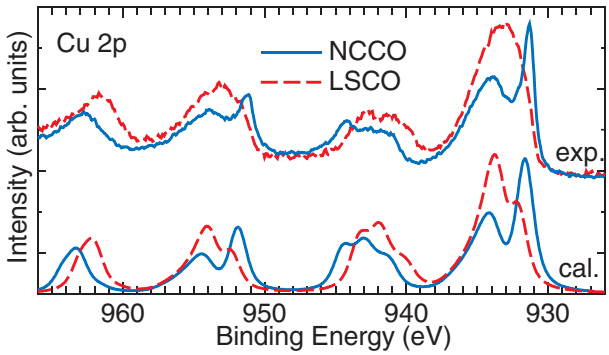

FIG. 3 (color online). IAM calculations for the Cu $2p$ core level PES of NCCO and LSCO (lower panel) compared with experiments (upper panel). The broad satellite around 944 eV is due to multiplets of $2p^5 3d^9$. The O $2p$ band width broadens the $2p^5 3d^{10}\underline{L}$ peak around 933.5 eV.

TABLE I. Estimated parameter values for NCCO and LSCO.

	Δ	Δ^*	U_{dd}	$U_{dc}(2p)$	$V(e_g)$	$V^*(e_g)$	T_{pp}	W_{lig}	W_{coh}
NCCO	3.0	0.25	8.0	10.5	3.5	1.8	1.0	4.0	0.5
LSCO	3.6	1.35	8.0	10.0	3.75	1.25	1.0	4.0	0.5

ever, this still does not explain the small CP shift of O 1s levels (+0.25 to −0.2 eV) from NCCO to LSCO. Using O 1s XAS to probe the unoccupied density of states, it is known that h doping in LSCO develops a new feature [30] below the UHB while e doping in NCCO results [31,32] in effectively enhancing the intensity of the UHB itself [Fig. 2(b)]. The results indicate that the onset peak position of the UHB for LSCO is 0.8–1.0 eV higher in energy than that of NCCO with respect to the O 1s core level [30–32].

Putting the O 1s HX-PES, O 1s XAS, and Cu 2p HX-PES data together in an energy level diagram, we arrive at the picture (Fig. 4) describing all the spectroscopic results: (i) The UHB of LSCO is higher in energy than that of NCCO, following the O 1s XAS. (ii) The difference in Δ^* is an approximate measure of the band gap of both NCO and LCO (∼1.0 eV) which is consistent with the resonant PES [14] and optical gap [17]. (iii) The CP shift between NCCO and LSCO is rather small compared with the optical gap, explaining the small peak shift in O 1s spectra compared to a crossing the gap picture. (iv) Fig. 4 clearly shows that e doping-induced states lie at or near the bottom of the UHB in NCCO while the h doping-induced states are situated near the top of the VB, separated by ∼1 eV. It is important to note that, in the midgap pinning scenario, Δ^* has to be the same value in both e and h doped systems and would result in the same spectral shape of Cu 2p for NCCO and LSCO.

In conclusion, bulk sensitive HX-PES is used to show that LSCO and NCCO exhibit new bulk character electronic states originating in screening from doped states, which are strongly suppressed within ∼15 Å of the surface. IAM calculations, complemented with O 1s XAS, explain the intriguingly small CP shift in core levels (∼0.2 eV for h or e doping in LSCO and NCCO) as well as valence and conduction band modifications spanning the band gap (∼1 eV). The IAM calculations cannot reproduce the ZRS feature observed in LCO, but which was predicted from MSCM with nonlocal screening in the absence of doping [11,12].

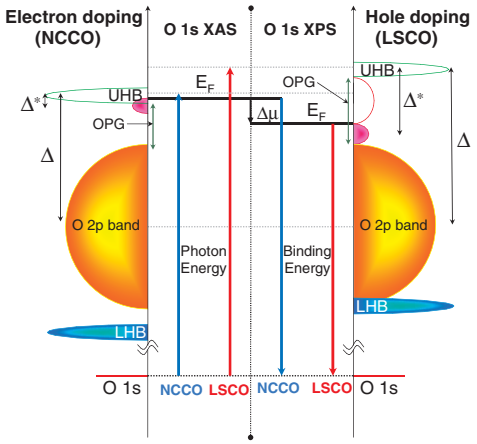

FIG. 4 (color). Schematic illustration of the energy levels of LSCO and NCCO obtained from the IAM analysis. OPG represents the optical gap in undoped materials. The Fermi level (E_F) separates the occupied density of states (shaded regions) from the unoccupied density of states.

This work was supported by the Ministry of Education, Science, Sports, and Culture through a Grant-in-Aid for Scientific Research (A) (No. 15206006), COE Research (No. 13CE2002) and an aid fund from ENERGIA.

[1] M. Imada *et al.*, Rev. Mod. Phys. **70**, 1039 (1998).
[2] P. A. Cox, *Transition Metal Oxides* (Clarendon, Oxford, 1992).
[3] *Practical Surface Analysis*, edited by D. Briggs and M. P. Seah (J. Wiley London, New York, 1990), 2nd ed..
[4] J. Zaanen *et al.*, Phys. Rev. Lett. **55**, 418 (1985).
[5] A. Fujimori *et al.*, Phys. Rev. B **35**, 8814 (1987).
[6] Z.-X. Shen *et al.*, Phys. Rev. B **36**, 8414 (1987).
[7] T. R. Cummins *et al.*, Phys. Rev. B **48**, 6556 (1993).
[8] A. Koitzsch *et al.*, Phys. Rev. B **66**, 024519 (2002).
[9] C. C. Tsuei *et al.*, Physica C (Amsterdam) **161**, 415 (1989).
[10] M. Gurvitch *et al.*, Phys. Rev. Lett. **59**, 1337 (1987).
[11] M. A. van Veenendaal *et al.*, Phys. Rev. B **47**, 11 462 (1993).
[12] M. A. van Veenendaal *et al.*, Phys. Rev. B **49**, 3473 (1994).
[13] H. Eskes *et al.*, Phys. Rev. Lett. **67**, 1035 (1991).
[14] P. G. Steeneken *et al.*, Phys. Rev. Lett. **90**, 247005 (2003).
[15] J. W. Allen *et al.*, Phys. Rev. Lett. **64**, 595 (1990).
[16] N. Harima *et al.*, Phys. Rev. B **64**, 220507(R) (2001).
[17] S. Uchida *et al.*, Phys. Rev. B **43**, 7942 (1991).
[18] G. Ghiringhelli *et al.*, Physica B (Amsterdam) **312–313**, 34 (2002).
[19] O. Tjernberg *et al.*, Phys. Rev. B **67**, 100501 (2003).
[20] I. Lindau *et al.*, Nature (London) **250**, 214 (1974).
[21] L. Braicovich *et al.*, Phys. Rev. B **56**, 15 047 (1997); C. Dallera *et al.*, ESRF Highlights, 77, (2001).
[22] K. Tamasaku *et al.*, Nucl. Instrum. Methods Phys. Res., Sect. A **467–468**, 686 (2001).
[23] K. Kobayashi *et al.*, Appl. Phys. Lett. **83**, 1005 (2003).
[24] M. Taguchi *et al.*, Phys. Rev. B **71**, 155102 (2005).
[25] K. Okada *et al.*, J. Electron Spectrosc. Relat. Phenom. **86**, 119 (1997).
[26] T. Boske *et al.*, Phys. Rev. B **56**, 3438 (1997).
[27] J. Ghijsen *et al.*, Phys. Rev. B **38**, 11 322 (1988).
[28] Y. Seino *et al.*, J. Phys. Soc. Jpn. **59**, 1384 (1990).
[29] K. Horiba *et al.*, Phys. Rev. Lett. **93**, 236401 (2004).
[30] C. T. Chen *et al.*, Phys. Rev. Lett. **66**, 104 (1991).
[31] M. Alexander *et al.*, Phys. Rev. B **43**, 333 (1991).
[32] J. Fink *et al.*, J. Electron Spectrosc. Relat. Phenom. **66**, 395 (1994).